Atmos. Chem. Phys. Discuss., https://doi.org/10.5194/acp-2018-386
Manuscript under review for journal Atmos. Chem. Phys.
Discussion started: 2 May 2018

Atmospheric Chemistry and Physics Discussions

Ice particle properties of Arctic cirrus

Veronika Wolf[1], Thomas Kuhn[1], Mathias Milz[1], Peter Voelger[2], Martina Krämer[3], and Christian Rolf[3]

[1]Luleå University of Technology, Division of Space Technology, Kiruna, Sweden
[2]Swedish Institute of Space Physics (IRF), Solar Terrestrial and Atmospheric Research Programme, Kiruna, Sweden
[3]Research Centre Jülich, Institute for Energy and Climate Research 7: Stratosphere (IEK-7), Jülich, Germany

Correspondence to: Veronika Wolf (Veronika.Wolf@ltu.se)

Abstract. Ice particle and cloud properties such as particle size, particle shape and number concentration influence the net radiation effect of cirrus clouds. Measurements of these features are of great interest for the improvement of weather and climate models, especially for the Arctic region. In this study, balloon-borne in-situ measurements of Arctic cirrus clouds have been analysed for the first time with respect to their origin. Eight cirrus cloud measurements were carried out in Kiruna (68° N), Sweden. Ice particle diameters between 10 μm and 1200 μm were found and the shape could be recognised from 20 μm upwards. Great variability in particle size and shape was observed. This cannot simply be explained by local environmental conditions. However, if sorted by cirrus origin, wind, and weather conditions, the observed differences can be assessed. Number concentrations between 3 / L and 400 / L were measured, but only for two cases the number concentration reached values above 100 / L. These two cirrus clouds were of in-situ origin and were caused by gravity and mountain lee-waves. For all other measurements, the maximum ice particle concentration was below 50 / L and for one in-situ origin cirrus case only 3 / L. In the case of in-situ origin clouds, the particles were all smaller than 350 μm diameter. The number size distribution for liquid origin clouds was much broader with particle sizes between 10 μm and 1200 μm. Furthermore, it is striking that in the case of in-situ origin clouds almost all particles were compact (61 %) or irregular (25 %) when examining the particle shape. In liquid origin clouds, on the other hand, most particles were irregular (48 %), rosettes (25 %) or columnar (14 %). There were hardly any plates in cirrus regardless of their origin. It is also noticeable that in the case of liquid origin clouds the rosettes and columnar particles were almost all hollow.

1 Introduction

Cirrus clouds have a great influence on the radiation balance of the Earth and thus also on the climate (Liou, 1986; Sassen and Comstock, 2001). However, despite decades of research there are still questions which are not fully answered (Potter and Cess, 2004; Boucher et al., 2013). This is mostly due to uncertainties in ice particle and cloud properties, such as particle size,

Atmos. Chem. Phys. Discuss., https://doi.org/10.5194/acp-2018-386
Manuscript under review for journal Atmos. Chem. Phys.
Discussion started: 2 May 2018

Atmospheric Chemistry and Physics Discussions

shape and number concentration. Depending on various particle and cloud properties, cirrus clouds can have a warming or also a cooling effect (Freeman and Liou, 1979; Liou, 1986; Platt, 1989; Kienast-Sjögren et al., 2016).

The Fourth Assessment Report of the Intergovernmental Panel on Climate Change (Solomon et al., 2007) points out that improved knowledge about cirrus clouds in the Arctic is a priority because the high latitudes are much more affected by climate change than other latitudes. Due to the remoteness of large parts of the Arctic region cirrus clouds there have been studied far less often than at other latitudes. Furthermore, most of the measuring campaigns in the Arctic have been aircraft measurements (e.g., Korolev et al., 1999; Garrett et al., 2001; Gayet et al., 2007) but not always especially dedicated to Arctic cirrus measurements. Particle sampling by aircraft suffered from shattering effects at the inlet of the instrument due to the high speed of the aircraft (e.g., Korolev et al., 2011, 2013; Jackson et al., 2014). This shattering led to incorrect size distributions with too many small particles. A new inlet design and algorithm might overcome this problem, at least partly (Korolev et al., 2013; Jackson et al., 2014). One advantage of balloon-borne measurements is that vertical cloud profiles can be measured with high spatial resolution. Furthermore, it is possible to measure with a very high image resolution.

Particle shape and size distribution information are important for a more precise parameterisation in models to better calculate the radiant fluxes, as described by Schlimme et al. (2005). A result of their study was that particle shape has a greater influence on the optical properties of the cloud than size distribution. In addition to shape and size distribution, also roughness and hollowness of the particles are of interest, as they also influence the optical properties, as described for example by Tang et al. (2017). Gu et al. (2011) confirmed that accurate knowledge of particle properties leads to better and more realistic parameterisations and can thus improve the retrievals for remote sensing methods as well as weather and climate models.

Therefore, this study discusses measurements of particle properties with a particular emphasis on particle shape and size. For this, we detect particles with a very high image resolution (1 pixel = 1.65 μm) so that the shape is identifiable from a size of 20μm upwards. On aircraft, in comparison, the often used optical array probes record the shadow of particles with pixel resolutions between 10 μm and 25 μm (Knollenberg, 1981; Lawson et al., 2006; Baumgardner et al., 2017). The cloud particle imager, CPI (Lawson et al., 2001) has at 2.3 μm a comparable pixel resolution so that it may be used for smaller particles, if they are in-focus.

The properties of ice clouds and particles depend on ambient conditions, such as front systems, waves, temperature, and humidity (e.g., Lynch, 2002; Spichtinger et al., 2005; Krämer et al., 2016). Several studies have shown how ice cloud properties depend on meteorological conditions, see Heymsfield et al. (2017) and references therein. In addition to considering the local environmental conditions, ice clouds may be classified and analysed in respect to conditions at their origin (Krämer et al., 2016; Wernli et al., 2016). Certain characteristic properties may then be attributed to one of two origin types, liquid origin or in-situ origin.

For these reasons, balloon-borne in-situ measurements have been carried out north of the Arctic Circle in Kiruna, in order to obtain high-resolution images of ice particles in cirrus clouds and thus provide accurate information on Arctic cirrus clouds, their particles, and properties. The measured cirrus clouds have been sorted according to their cloud origin, the meteorological situation, and the wind direction. The analysis focuses on ice particle and cloud properties in relation to these conditions. The

following sections describe the measurements and the instruments used. The collected data are then presented, analysed and discussed. Finally, the results are summarized

2 Campaign Description

2.1 Location

Balloon-borne in-situ cirrus measurements have been carried out at Esrange Space Centre (ESRANGE), which is a rocket range and research centre 40 km east of Kiruna. Kiruna (68° N, 20° E) has a subarctic climate as it is located north of the Arctic Circle and east of the Scandinavian Mountains. All measurement days are in the winter season between the end of November and the beginning of April. Above ESRANGE during this time of the year, the minimum temperature in the troposphere is between $-70°$ C and $-55°$ C.

2.2 Measurement methods

For the measurement of cloud and particle properties, an in-situ imager and radiosondes are utilised. Auxiliary data from two LIDARs, one located at Swedish Institute of Space Physics (IRF, Kiruna) and one at ESRANGE, as well as a RADAR located at ESRANGE are also used. The heart of these measurements is the in-situ imager. This device with related methods and the instruments to support the measurements are described in this section.

2.2.1 In-situ imager

The self-built in-situ imager is described in detail by Kuhn et al. (2013) and Kuhn and Heymsfield (2016). Figure 1 shows the top view of the open device (covers removed). The instrument consists of two main parts: one for battery, camera (label c) in Fig.1), motor (d) and computer (e); and another part for collecting ice particles with inlet (a), oil-coated film (b), and optics. Particles enter the imager through the inlet and fall onto the oil coated tape. The tape is moving at constant speed to avoid superposition of particles. Shortly after it passed the inlet, the tape is photographed by a CCD camera and the images are stored on a memory disk. The particle imager samples ice particles along the trajectory of the ascending balloon. At a height of about 13 km, the instrument is cut off from the balloon and descends with a parachute. All measurements have been carried out when the ground is covered by snow and the lakes are frozen. This allows a safe landing and easy recovery by helicopter. After the recovery of the imager, the images are evaluated on the computer, partly manually and partly automatically.

Once the particle outlines have been traced, particle size, shape, area, and number concentration can be determined automatically. The CCD camera and optics enable high-resolution images of ice particles, 1 pixel corresponds to 1.65 μm. This allows us to identify shapes of particles with sizes of 20 μm or larger. As a measure of ice particle size, we use the maximum dimension (Dmax) i.e. the smallest diameter of the circle that encloses the whole particle. The ice particles are classified into shapes by looking at each individual ice particle and assigning it to one of five shape groups: *compact*, *irregular*, *rosettes*, *plates*, and *columnar* particles. These groups were defined based on a classification by Bailey and Hallett (2009). Figure 2 shows

cases of each group. Compact particles are spheroidal. Rosettes include all types of bullet rosettes, column rosettes, sheath rosettes and irregular rosettes. Rosettes can have two or more arms. Plates and columnar particles are symmetrical with simple hexagonal geometries. They will most likely attach to the oil-coated tape with one of their facets having the longest dimension. Thus, we classify particles visible with a hexagonal basal facet as plates and ice particles that show the longer prism facets as columnar. In addition to hexagonal columns, the shape group of columnar particles also includes single bullets. Irregulars are those particles that cannot be sorted into any other group. For each measured cirrus cloud, all particles were assigned to one of the five shape groups. For each measured cirrus cloud, the frequency of occurrence of shapes is determined as percentages corresponding to the five particle shape groups.

The vertical resolution of particle concentration and size distributions depend on the number of collected particles. In case of high particle concentration, averaging over 10 s is sufficient, which corresponds to around 60 m. For the size distributions, a slightly higher averaging period has to be used. If the particle concentration is low, the size distribution over the whole cloud must be averaged. This results in different vertical resolutions for particle concentration and size distributions at the different measurement flights.

2.2.2 Radiosonde, LIDARs and RADAR

During flight a radiosonde is attached to the in-situ imager. With the help of the radiosonde data, temperature, humidity, height and geographical coordinates can be assigned to each particle. The RS92 from Väisälä is used for these measurements. If available, the data from parallel observations by a RADAR and two LIDARs located in Kiruna and surrounding are also used. ESRAD, an atmospheric Mesosphere-Stratosphere-Troposphere RADAR (Kirkwood et al., 2007) located at ESRANGE provides information on the dynamic state of the atmosphere, winds, and waves. Whenever LIDAR measurements are possible, these are used to complement the in-situ balloon-borne measurements. One LIDAR is located at the Swedish Institute of Space Physics (IRF) (about 30 km away from ESRANGE) and another one is located at ESRANGE close to the balloon launch pad. The LIDAR at IRF (Voelger and Nikulin, 2005) is an elastic backscatter LIDAR and at ESRANGE a Raman-Mie LIDAR (Blum and Fricke, 2005). The backscattered signal is used in this study to observe the evolution of the cloud over time. A comparison of the extinction derived from LIDAR and the in-situ imager has been published elsewhere (Kuhn et al., 2017).

3 Classification of measurements

Data from eight measurement flights are presented in this study. In Tab. 1 the flight times of the balloons and data are listed. The following sections describe the classification of the clouds probed on these eight days in terms of their formation origin, weather conditions and cloud properties. Tab. 1 shows each measured cirrus with corresponding classification.

3.1 Cirrus origin

A simple and quite new method of classifying clouds is based on their origin. Two possible cirrus origins are distinguished, *liquid* and *in-situ*. This classification is described in detail by Krämer et al. (2016) and Luebke et al. (2016) and is briefly

Atmos. Chem. Phys. Discuss., https://doi.org/10.5194/acp-2018-386
Manuscript under review for journal Atmos. Chem. Phys.
Discussion started: 2 May 2018

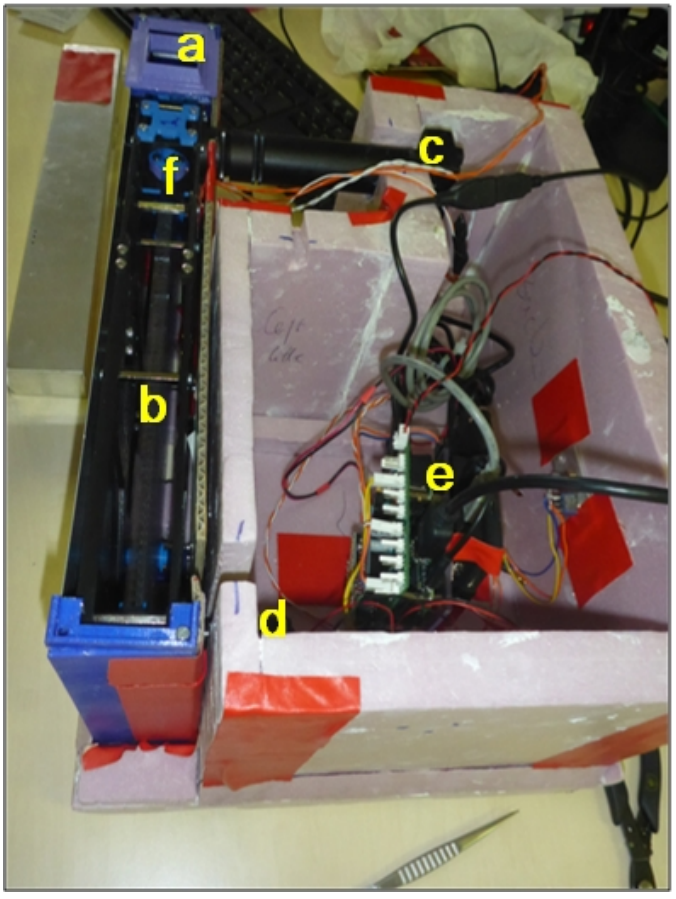

Figure 1. Top view on the open in-situ imager. a) inlet where particles enter during measurement. b) oil coated moving film. c) CCD camera with an objective takes grey-map pictures every 1s. d) Motor which moves the film. e) Computer and battery f) LED to illuminate the film.

Table 1. List of measurement days, launch and cut-off times, cloud origins and meteorological situations

date	start time (UTC)	cut off (UTC)	origin	meteorological situation	wind direction	waves
2012-04-04	12:09	13:08	in-situ	occlusion	NW	waves
2013-02-20	11:15	12:17	in-situ	orographic/ before cold front	NW	waves
2013-12-18	10:45	11:46	liquid	occlusion	NW	waves
2014-03-20	12:39	13:42	liquid	warm front	NW	no waves
2015-04-01	09:40	10:34	liquid	low pressure center/ after occlusion	SSW	no waves
2016-02-12	09:38	10:42	liquid	warm front	SSW	no waves
2016-03-15	08:26	09:38	in-situ	orographic/ before cold front	NW	waves
2016-12-15	10:03	11:04	in-situ	occlusion	NW	no waves

Atmos. Chem. Phys. Discuss., https://doi.org/10.5194/acp-2018-386
Manuscript under review for journal Atmos. Chem. Phys.
Discussion started: 2 May 2018

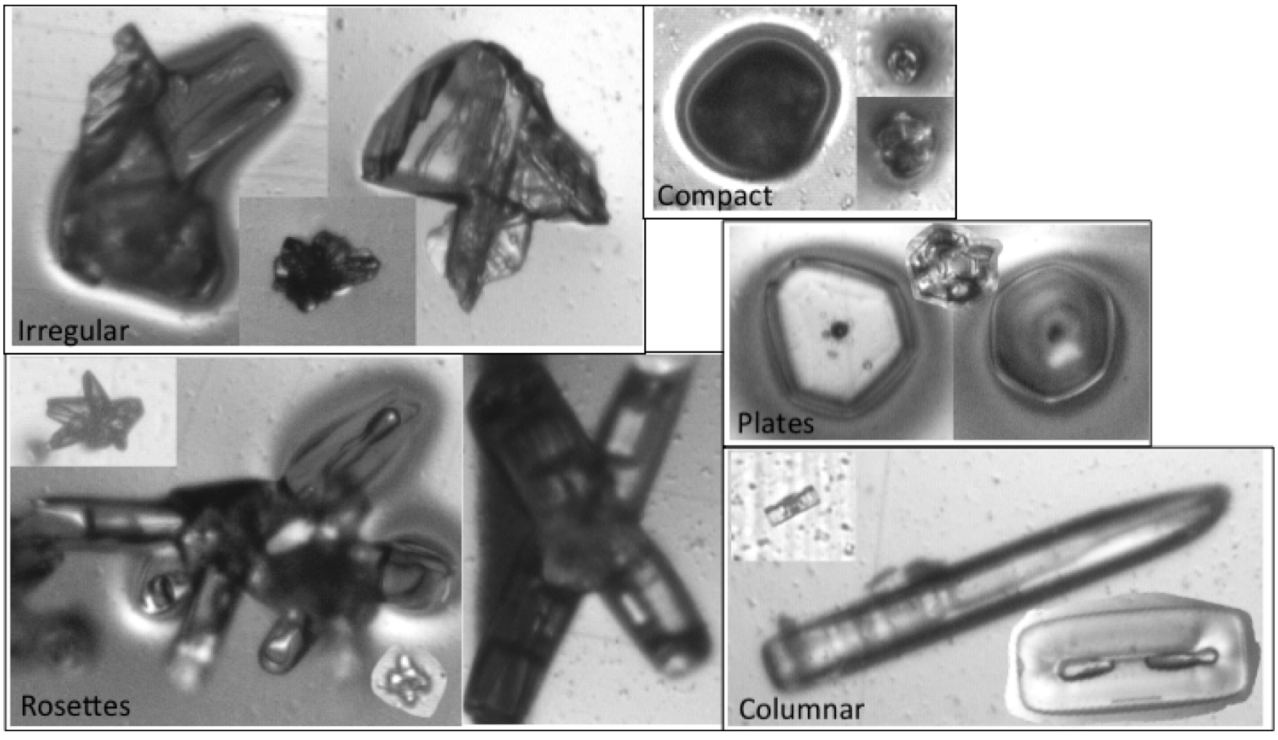

Figure 2. Classification of the different particles into five shape groups, which are: compact, irregular, columnar, plates, and rosettes.

outlined in the following. If the cloud was formed at a temperature below 235 K, it is assumed to be an in-situ origin cloud, in which particles form directly from the gaseous phase to the solid phase. If the temperature at the formation of the cloud was above 235 K, it is considered to be a liquid origin cloud. In this case the ice particles formed at lower altitudes via the liquid phase and were lifted subsequently to the cirrus temperature range. As formation in this context we consider the time when the ice water content (IWC) started to be greater than zero, or 24 h before the in-situ measurement in case IWC > 0 during these 24 h. Consequently, the cirrus origin was determined here using temperature and IWC along 24 h back trajectories. The Lagrangian microphysical model CLaMS-Ice (Luebke et al., 2016) was used to calculate these trajectories, starting from locations along the balloon flight paths, based on ECMWF ERA-Interim meteorological fields. Temperature was interpolated onto the trajectories, while the IWC was simulated with CLaMS-Ice before the balloon measurement. The resulting classifications are listed in Tab. 1. Half of the measured cirrus clouds are classified as in-situ origin, the other half as liquid origin.

3.2 Weather conditions

Weather conditions are analysed using weather maps and satellite images. The wind direction is ascertained with the help of the balloon trajectories and the back trajectories of the air mass. Figure 3 shows the back trajectories of air parcels at average cloud heights for 24 h before the flight (left) and the trajectories of the in-situ imager flights (right). It can be seen that the

Atmos. Chem. Phys. Discuss., https://doi.org/10.5194/acp-2018-386
Manuscript under review for journal Atmos. Chem. Phys.
Discussion started: 2 May 2018

wind came from the south only on two of eight days. On all other days, the wind direction was north-west and thus over the Scandinavian Mountains. In this case, mountain lee-waves or gravity waves can occur. Indications for this have been observed by ESRAD on four days. The cirrus was caused four times in context with an occlusion and twice in relation to a warm front. Twice the Cirrus was formed in front of a cold front due to strong wind and orographic uplift over the Scandinavian Mountains.

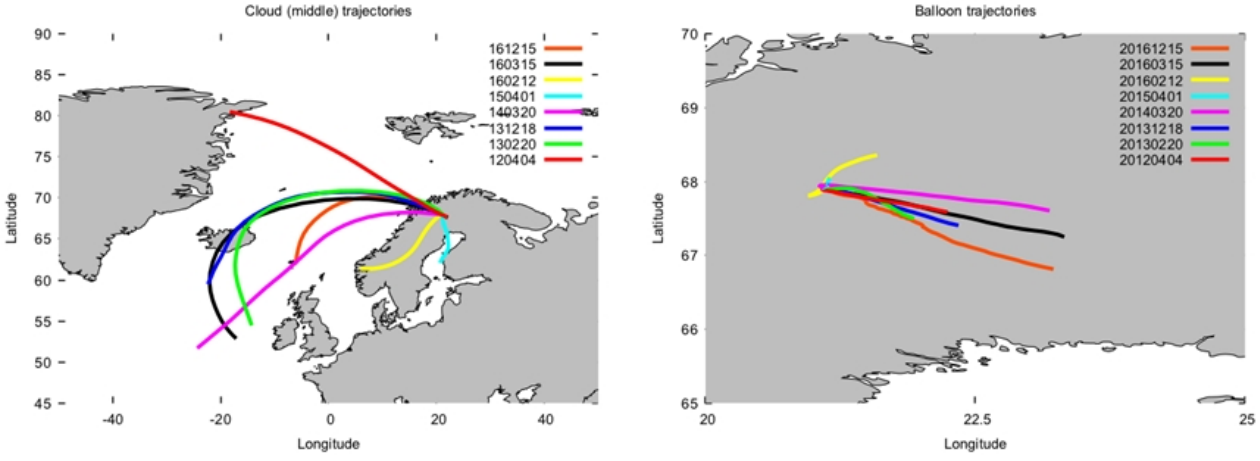

Figure 3. On the left the 24 h back trajectories of the average cloud height air mass for all days are shown and on the right the trajectories of the balloon measurements. The airmass back trajectories latitudes and longitudes are calculated by CLaMS. The balloon coordinates were measured by the RS92 sonde.

3.3 Cloud properties

For all observations, particle size ranges, number concentration and mean temperature for different cloud levels are listed in Tab. 2. The lower altitude of the first cloud level and the upper altitude of the last cloud level define the total extent of the cloud. Two cirrus clouds (1.4.2015 and 12.2.2016) had a vertical extension of approximately 6 km with a low cloud base at an altitude of 2 km and 3 km, respectively. The other six cirrus clouds were thinner (80 m – 2 km thick) and had a higher cloud base (over 6 km). In all cases the temperatures decreased with altitude. The temperatures at the cloud tops were between -60° C and -70° C. At the cloud base, the temperatures were between -45° C and -55° C in case of thin clouds and between -10° C and -20° C in case of the two thick clouds. The relative humidity with respect to ice in the clouds was between 80% and 130%. Particles with sizes between 10 μm and 1200 μm were collected. Smaller particles are not efficiently sampled (Kuhn and Heymsfield, 2016), and larger particles have not been encountered. Table 2 lists the size ranges for each cloud. The ice particle number concentrations were between (3 / L) and (400 / L). For each measured cirrus cloud, the frequency of occurrence of shapes is summarized in Tab. 3 as percentages corresponding to the five particle shape groups compact, irregular, rosettes, plates and columnar. Some images of the particles from each measurement are shown in Fig. 4. All particle images are shown with the same size scaling.

Atmos. Chem. Phys. Discuss., https://doi.org/10.5194/acp-2018-386
Manuscript under review for journal Atmos. Chem. Phys.
Discussion started: 2 May 2018

Atmospheric Chemistry and Physics Discussions

Table 2. Cloud altitude level, mean temperature, maximum dimension Dmax (minimum, maximum, median) and mean number concentration

Date - origin	level min/max m	T °C	Dmax min/ median/ max μm	NC 1/L
4.4.2012 - in-situ	5550/ 5680	-42.4	36/ 81/ 172	8
	5680/ 6540	-45.5	28/ 155/ 230	4
	6630/ 6860	-51.8	51/ 137/ 327	11
	6860/ 6940	-53.1	24/ 81/ 176	32
	7030/ 7270	-54.5	7/ 29/ 137	131
20.2.2013 - in-situ	8980/ 9340	-57.8	24/ 47/ 91	86
	9660/ 9900	-62.8	14/ 31/ 78	225
	10080/ 10440	-66.3	15/ 24/ 57	373
18.12.2013 - liquid	7960/ 8050	-52.6	24/ 84/ 277	16
20.3.2014 - liquid	6020/ 6240	-36.2	35/ 180/ 492	11
	8260/ 8330	-54.4	16/ 66/ 222	56
	8550/ 8630	-57.2	11/ 59/ 203	46
1.4.2015 - liquid	1940/ 2450	-11.5	87/ 222/ 415	2
	5850/ 6080	-37.2	26/ 256/ 643	7
	7720/ 8410	-54	22/ 126/ 389	15
12.2.2016 - liquid	3400/ 4520	-25.8	68/ 229/ 693	4
	4530/ 5560	-30.2	55/ 233/ 1105	13
	5570/ 7680	-40.5	68/ 296/ 1116	5
	7570/ 10640	-58.4	5/ 218/ 1228	3
15.3.2016 - in-situ	8950/ 9390	-48.8	25/ 38/ 105	14
	10980/ 11550	-64.1	25/ 43/ 97	11
15.12.2016 - in-situ	10120/ 11750	-65.5	25/ 52/ 102	3

Atmos. Chem. Phys. Discuss., https://doi.org/10.5194/acp-2018-386
Manuscript under review for journal Atmos. Chem. Phys.
Discussion started: 2 May 2018

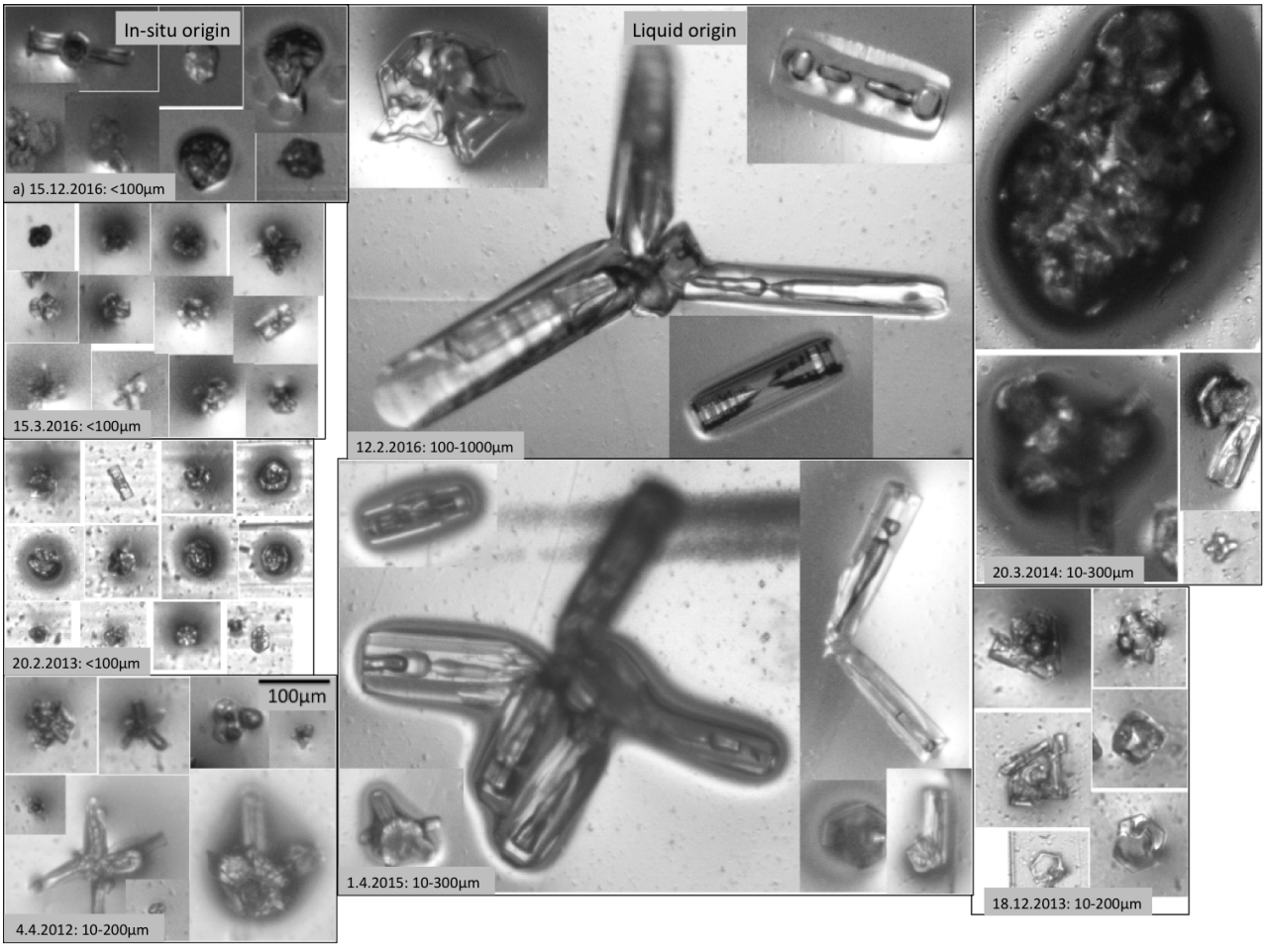

Figure 4. Some pictures of ice particles from all measurement days. The left panel shows ice particles from in-situ origin cirrus, on the right liquid origin crystals are displayed. For a better understanding of the size, a 100 μm bar is displayed (4.4.2012 bottom). All images have the same scale resolution and 100 μm corresponds to 61 pixel.

Atmos. Chem. Phys. Discuss., https://doi.org/10.5194/acp-2018-386
Manuscript under review for journal Atmos. Chem. Phys.
Discussion started: 2 May 2018

Atmospheric Chemistry and Physics Discussions

Table 3. List of days and relative number (in %) of particles in different shape groups.

Date - origin	compact	irregulars	rosettes	plates	columnar
4.4.2012 - in-situ	38.8	42.2	16.5	0.4	2.2
20.2.2013 - in-situ	71.7	19.4	2.5	1.8	4.7
18.12.2013 - liquid	4.3	69.6	6.5	8.7	10.9
20.3.2014 - liquid	27.2	60.8	9.5	0.3	2.2
1.4.2015 - liquid	4.5	21.2	54.8	1.4	18.2
12.2.2016 - liquid	6.0	39.2	28.5	3.8	22.6
15.3.2016 - in-situ	72.4	21.3	4.7	0.7	1.0
15.12.2016 - in-situ	63.9	16.8	4.2	0.0	15.1

4 Results and Discussion

4.1 Size and number concentration

On two days (1.4.2015 and 12.2.2016, see observations 2) we collected very large ice particles, with maximum sizes of approximately 600 μm and 1200 μm respectively. Both days represent two liquid origin cases with southerly winds, low cloud base, and large vertical extension. In cases of in-situ origin cirrus, all particles were smaller than 350 μm. At three of the four days (20.2.2013, 15.3.2016 and 15.12.2016) all particles were even smaller than 100 μm. This difference in size is also reflected in the number size distribution. As examples, Fig. 5 shows the number size distributions from two days, one with an in-situ origin cloud shown in red (20.2.2013) and one with a liquid origin cloud shown in blue (12.2.2016). For each cloud, three size distributions are shown from different heights within the cloud. All distributions of the liquid-origin cloud extend to larger sizes and are much broader than in the case of the in-situ origin. Data from our other launches, which are not shown here, confirm this observation. In general, the number size distributions are more narrow with increasing height and lower temperature. This can be clearly seen, for example, for the in-situ origin cloud in Fig. 5. However, these variations are less than the general differences observed between in-situ origin and liquid origin. Thus, the broadest size distribution at the lowest height of the in-situ origin cloud on 20.2.2013 is still much more narrow than any distribution of the liquid-origin cloud on 12.2.2016. This means, that size distributions measured in different clouds but at similar altitudes and temperatures can be vastly different. While these differences are obviously not related to the local ambient conditions, they are related to the cloud origin.

Data reported earlier from aircraft measurement at high latitudes also show a large range in sizes (e.g., Gayet et al., 2007) comparable to the observations of our balloon measurements. So far, only Krämer et al. (2016) and Luebke et al. (2016) investigated the dependence of size on cloud origin for mid-latitude spring cirrus. For Arctic cirrus, our observations corroborate their findings that in-situ origin clouds contain smaller particles than liquid-origin clouds. Furthermore, one can recognize in the number size distributions in Fig. 5 that in the case of the in-situ origin cirrus cloud, the number concentration was many times higher than in the liquid origin cloud. It should be noted that the y-axis is logarithmic, so that size distributions for both cases can be seen despite this large difference in concentration.

The total number concentrations are shown in Fig. 6 as altitude profiles for the same two days (red 20.2.2013 in-situ origin and blue 12.2.2016 liquid origin). In these two cases, the concentration of the in-situ origin cloud was 15 to 20 times greater than in the liquid origin cloud. This much higher number concentration in the case of this in-situ origin cloud does not apply to all of our in-situ origin cases, but only to two measurements (20.2.2013 and 15.3.2016). Krämer et al. (2016) discussed two types of in-situ origin cirrus. The first type appears in slow updrafts, e. g. in warm conveyor belts. The ice is nucleated mostly heterogeneously and the corresponding ice particle number concentrations are low. In the second type which is related to fast updrafts, the ice particles form homogeneously with high number concentrations triggered by the fast updraft. These two days with higher number concentration (300 -400 / L) were associated to very strong wind coming from the northwest which led to waves, as was observed by ESRAD on both days. For one day Fig. 7 shows the LIDAR extinction coefficient from 20.2.2013 (left) and the ESRAD vertical velocity (right). These gravity or mountain lee waves with the related high vertical velocities can explain such higher number concentrations. The other two in-situ origin clouds had lower number concentrations, and one of them (15.12.2016) had with 3 / L the lowest concentration of our eight balloon flights. The concentrations for liquid origin clouds were always relatively low (5 / L to 70 / L). Since liquid-origin clouds were formed at warmer temperatures, they are originally nucleated heterogeneously from liquid drops. The lower number concentration in comparison to Luebke et al. (2016), who found a median ice number concentration slightly above 100 / L in liquid origin mid-latitude cirrus - might be due to a lower number of ice nucleating particles (INP) which are necessary for heterogeneous freezing in Arctic rgiond, (Costa et al., 2017). However, low number concentrations could also be caused by a dissolving cloud state. To confirm this, one would need INP or humidity measurements during some time before our measurements, hence, we can only speculate here.

4.2 Shape

Shape detection is sometimes intricate, even with high image resolution. Some particle shapes may be confusing, as also observed by others (e.g., Lindqvist et al., 2012). Here, the assignment between irregulars and rosettes was sometimes ambiguous, because in a few cases rosettes appear somewhat irregular. For example, some rosettes look as if they have a part missing or one bullet seems to be a longer column. In such cases, we have assigned these irregular rosettes to the shape group rosettes rather than to irregulars. In other cases, small compact ice particles sometimes show characteristics that indicate an initial formation of rosettes, however, we have still classified them as compact due to their spheroidal shape. Classifying them as rosettes would not have changed any of the results discussed here.

Despite these ambiguities, it is noticeable that the frequency of occurrence of the different particle shapes (see Tab. 3) varies depending on cloud origin. The average frequencies of shape occurrence for in-situ origin and for liquid origin clouds are shown in Fig. 8 (left panel). The right panel of this figure shows how the average particle sizes of the different shapes vary depending on the cloud origin. In both origin cases, plates were rarely collected.

As can be seen in Fig. 4 and Fig. 8, in the case of in-situ origin, the particles are usually small in size and compact or irregular in shape. However, in the case of liquid origin, the particles are most commonly irregular and rosettes. An explanation could be that a liquid origin cirrus forms at warmer temperatures with higher water vapour content in the air. Therefore, the ice particles are larger and can grow up to more complex shapes. This is especially the case on the two days (1.4.2015 and 12.2.2016) with

Atmos. Chem. Phys. Discuss., https://doi.org/10.5194/acp-2018-386
Manuscript under review for journal Atmos. Chem. Phys.
Discussion started: 2 May 2018

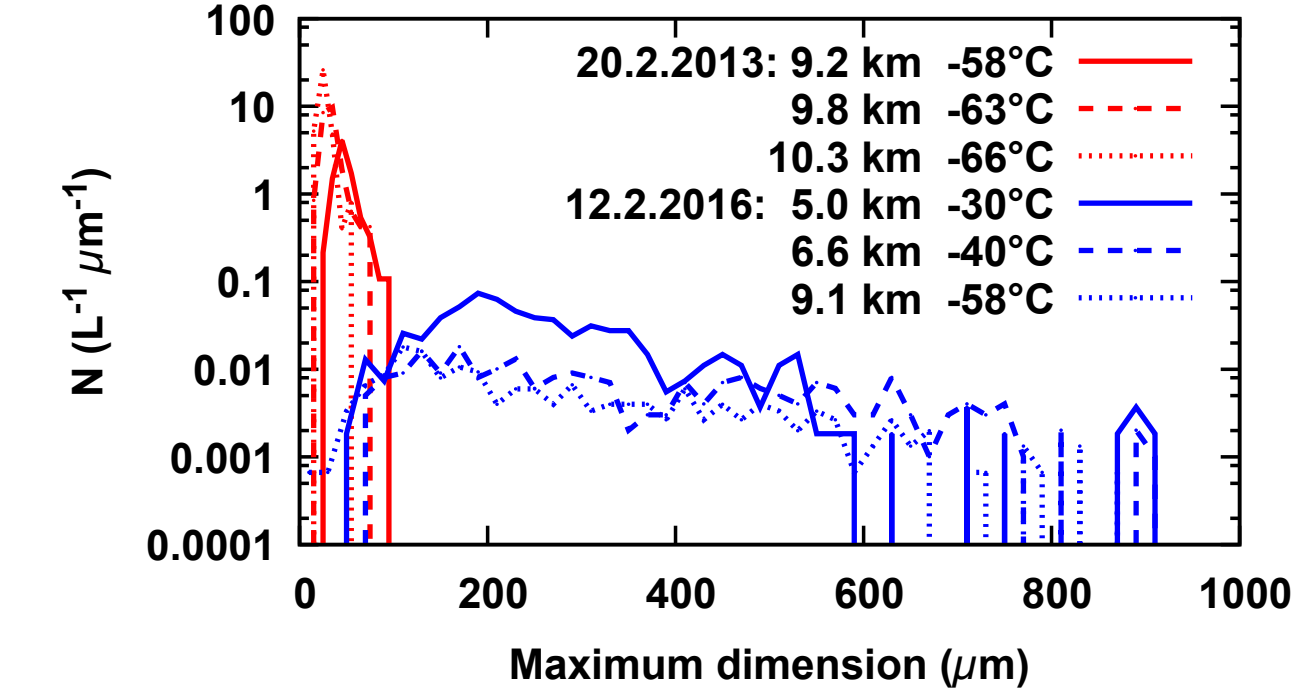

Figure 5. Number size distribution for two measurement days (20.2.2013, in-situ origin and 12.2.2016, liquid origin) for different cloud levels.

the particularly large ice particles where the lower cloud range was in the temperature regime of mixed-phase clouds. At the time of measurement, these two clouds were completely frozen. Hence, the liquid water, which was probably present at some earlier stage, has contributed to the observed extensive growth.

Compact particles are on average the smallest ones. The larger particles were rosettes, irregular or columnar particles. It is noticeable that almost all columnar particles and rosettes are hollow in case of liquid origin cirrus. This corroborates findings by others (e.g., Weickmann et al., 1948; Heymsfield et al., 2002; Schmitt et al., 2006). In the case of in-situ origin cirrus there are very few and if then very small rosettes and columns thus a statement regarding their hollowness is rather speculative. Like Korolev et al. (1999), we have collected only a few columnar particles and plates. They have collected only 3 % of such particles and we have gathered 8 %. Also, in the case of liquid origin these particle shapes were more frequent than in the case of in-situ origin.

Atmos. Chem. Phys. Discuss., https://doi.org/10.5194/acp-2018-386
Manuscript under review for journal Atmos. Chem. Phys.
Discussion started: 2 May 2018

Atmospheric Chemistry and Physics Discussions

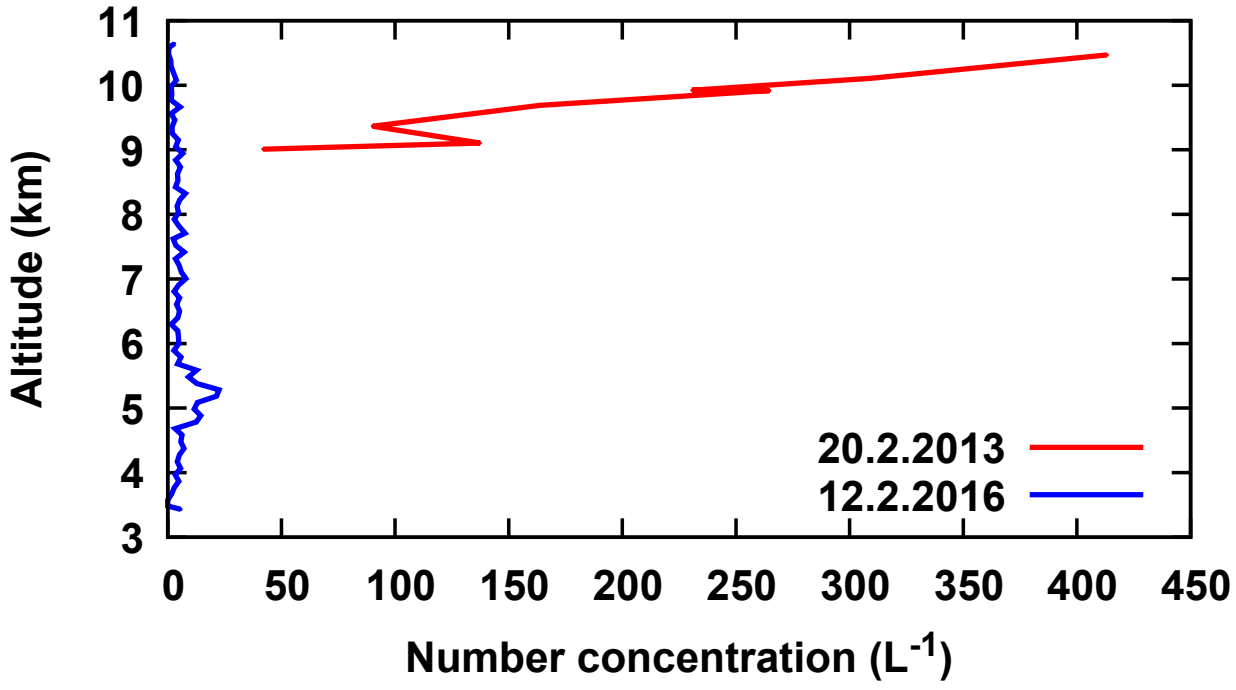

Figure 6. Number concentration as a function of altitude for two days (20.2.2013, in-situ origin and 12.2.2016, liquid origin)

5 Conclusions

In this study, eight balloon-borne in-situ measurements of Arctic cirrus clouds were analysed. The balloons were launched from Kiruna, Sweden during winter time. Particular emphasis was placed on the analysis of ice particle size, shape and number concentration with respect to cirrus origin. Since in-situ origin clouds are formed from the gas phase at temperatures below 235 K, while liquid origin clouds formed via liquid drops at temperatures above 235 K, the cloud and particle properties are expected to vary. In the case of our measurements, large differences in ice particle size, shape and number concentration are observed. However, when looking at the cirrus in terms of its origin, similarities between the various properties are striking. This implies that remote sensing retrievals and weather and climate models could be improved when accounting for these differences rather than using parameterisations that depend only on local conditions.

The most important results are summarized here:

1. Particle size: Arctic cirrus clouds with particle sizes between 10 μm and 1200 μm have been observed. Most common in our clouds are particles with sizes between 30 μm and 250 μm. While in-situ origin clouds have smaller particles with sizes below 350 μm, liquid origin clouds exhibit larger particles and wider number size distributions. The ice particles of

Atmos. Chem. Phys. Discuss., https://doi.org/10.5194/acp-2018-386
Manuscript under review for journal Atmos. Chem. Phys.
Discussion started: 2 May 2018

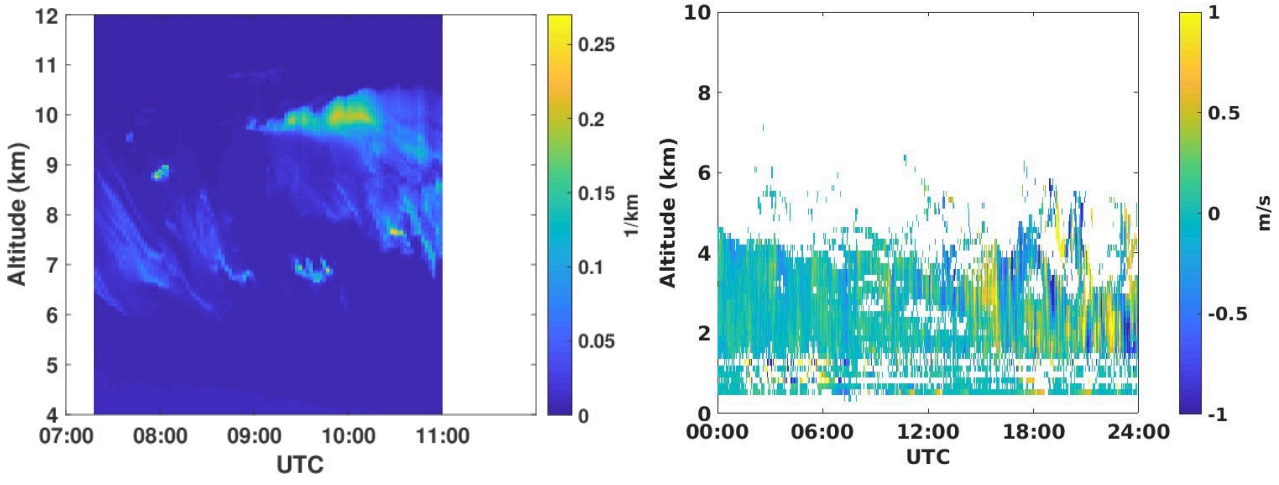

Figure 7. Extinction coefficient (left) derived from IRF LIDAR and vertical velocity (right) obtained from ESRAD for 20.2.2013 .

clouds with wind from the south are much larger and fewer than ice particles from the west where the cirrus was probably triggered by strong updrafts associated with gravity or mountain lee waves behind the Scandinavian Mountains.

2. Particle shape: The in-situ origin clouds consisted mainly of compact and irregular particles and the liquid origin clouds of irregular, rosettes and columns. In both cases, there are hardly any plates. The compact particles were the smallest particles and rosettes were the largest. Rosettes and columns were mostly hollow.

3. Particle number: The measured number concentrations were between 3 / L and 400 / L. Both extreme values were determined for in-situ origin clouds. The highest concentrations occurred due to waves on the lee side of the Scandinavian Mountains. Concentrations for liquid origin clouds were low (5 / L to 70 / L).

Future work will include more measurements for further significant statistical evaluation. In addition, we also want to allow several in-situ imagers to fly one after the other in order to investigate a temporal development of the particle properties.

Acknowledgements. We thank Peter Dalin (IRF) and Evgenia Belova (IRF) for interpreting and discussing the ESRAD data in terms of gravity and mountain lee-waves. We thank the Swedish National Space Board for funding these balloon campaigns (Grants Dnr 85/10, Dnr 86/11, Dnr 143/12, Dnr 273/12, Dnr 168/13, Dnr 124/14).

Atmos. Chem. Phys. Discuss., https://doi.org/10.5194/acp-2018-386
Manuscript under review for journal Atmos. Chem. Phys.
Discussion started: 2 May 2018

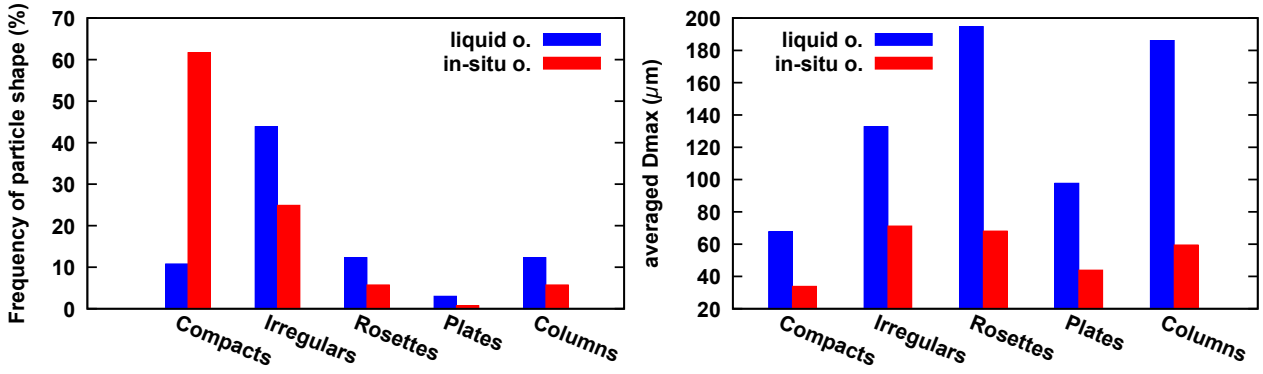

Figure 8. Occurrence of different particle shapes depending on cloud origin (left) and average Dmax for the different shapes (right). Mean values of shape and size of the four in-situ origin (red) measurements and four liquid origin (blue) measurements.

References

Bailey, M. P. and Hallett, J.: A comprehensive habit diagram for atmospheric ice crystals: Confirmation from the laboratory, AIRS II, and other field studies, Journal of the Atmospheric Sciences, 66, 2888–2899, https://doi.org/10.1175/2009JAS2883.1, 2009.

Baumgardner, D., Abel, S. J., Axisa, D., Cotton, R., Crosier, J., Field, P., Gurganus, C., Heymsfield, A., Korolev, A., Krämer, M., Lawson, P., McFarquhar, G., Ulanowski, Z., and Um, J.: Cloud Ice Properties: In Situ Measurement Challenges, Meteorological Monographs, 58, 9.1–9.23, https://doi.org/10.1175/AMSMONOGRAPHS-D-16-0011.1, https://doi.org/10.1175/AMSMONOGRAPHS-D-16-0011.1, 2017.

Blum, U. and Fricke, K. H.: The Bonn University lidar at the Esrange: Technical description and capabilities for atmospheric research, Annales Geophysicae, 23, 1645–1658, https://doi.org/10.5194/angeo-23-1645-2005, 2005.

Boucher, O., Randall, D., Artaxo, P., Bretherton, C., Feingold, G., Forster, P., Kerminen, V.-M., Kondo, Y., Liao, H., Lohmann, U., Rasch, P., Satheesh, S., Sherwood, S., Stevens, B., and Zhang, X.: Clouds and Aerosols. In: Climate Change 2013: The Physical Science Basis. Contribution of Working Group I to the Fifth Assessment Report of the Intergovernmental Panel on Climate Change [Stocker, T.F., D. Qin, G.-K. Plattner, M. Tignor, S.K. Allen, J. Boschung, A. Nauels, Y. Xia, V. Bex and P.M. Midgley (eds.)].nbsp;, 2013.

Costa, A., Meyer, J., Afchine, A., Luebke, A., Günther, G., Dorsey, J. R., Gallagher, M. W., Ehrlich, A., Wendisch, M., Baumgardner, D., Wex, H., and Krämer, M.: Classification of Arctic, midlatitude and tropical clouds in the mixed-phase temperature regime, Atmospheric Chem-

istry and Physics, 17, 12 219–12 238, https://doi.org/10.5194/acp-17-12219-2017, https://www.atmos-chem-phys.net/17/12219/2017/, 2017.

Freeman, K. P. and Liou, K.: Climatic effects of cirrus clouds., Advances in geophysics: volume 21, pp. 231–288, 1979.

Garrett, T. J., Hobbs, P. V., and Gerber, H.: Shortwave, singlescattering properties of arctic ice clouds, Journal of Geophysical Research: Atmospheres, 106, 15 155–15 172, https://doi.org/10.1029/2000JD900195, https://agupubs.onlinelibrary.wiley.com/doi/abs/10.1029/2000JD900195, 2001.

Gayet, J. F., Stachlewska, I. S., Jourdan, O., Shcherbakov, V., Schwarzenboeck, A., and Neuber, R.: Microphysical and optical properties of precipitating drizzle and ice particles obtained from alternated lidar and in situ measurements, Annales Geophysicae, 25, 1487–1497, 2007.

Gu, Y., Liou, K. N., Ou, S. C., and Fovell, R.: Cirrus cloud simulations using WRF with improved radiation parameterization and increased vertical resolution, Journal of Geophysical Research Atmospheres, 116, https://doi.org/10.1029/2010JD014574, 2011.

Heymsfield, A., Krämer, M., Wood, N. B., Gettelman, A., Field, P. R., and Liu, G.: Dependence of the Ice Water Content and Snowfall Rate on Temperature, Globally: Comparison of in Situ Observations, Satellite Active Remote Sensing Retrievals, and Global Climate Model Simulations, Journal of Applied Meteorology and Climatology, 56, 189–215, https://doi.org/10.1175/JAMC-D-16-0230.1, https://doi.org/10.1175/JAMC-D-16-0230.1, 2017.

Heymsfield, A. J., Lewis, S., Bansemer, A., Iaquinta, J., Miloshevich, L. M., Kajikawa, M., Twohy, C., and Poellot, M. R.: A general approach for deriving the properties of cirrus and stratiform ice cloud particles, Journal of the Atmospheric Sciences, 59, 3–29, 2002.

Jackson, R. C., Mcfarquhar, G. M., Stith, J., Beals, M., Shaw, R. A., Jensen, J., Fugal, J., and Korolev, A.: An assessment of the impact of antishattering tips and artifact removal techniques on cloud ice size distributions measured by the 2D cloud probe, Journal of Atmospheric and Oceanic Technology, 31, 2567–2590, https://doi.org/10.1175/JTECH-D-13-00239.1, 2014.

Kienast-Sjögren, E., Rolf, C., Seifert, P., Krieger, U. K., Luo, B. P., Krämer, M., and Peter, T.: Climatological and radiative properties of midlatitude cirrus clouds derived by automatic evaluation of lidar measurements, Atmos. Chem. Phys., pp. 7605–7621, https://doi.org/https://doi.org/10.5194/acp-16-7605-2016, 2016.

Kirkwood, S., Wolf, I., Nilsson, H., Dalin, P., Mikhaylova, D., and Belova, E.: Polar mesosphere summer echoes at Wasa, Antarctica (73S): First observations and comparison with 68N, Geophysical Research Letters, 34, https://doi.org/10.1029/2007GL030516, 2007.

Knollenberg, R. G.: Techniques for probing cloud microstructure. Clouds, Their Formation, Optical Properties and Effects, P. V. Hobbs and VDeepack (EDS.), Acadamic Press, pp. 15–91, 1981.

Korolev, A., Emery, E., and Creelman, K.: Modification and tests of particle probe tips to mitigate effects of ice shattering, Journal of Atmospheric and Oceanic Technology, 30, 690–708, https://doi.org/10.1175/JTECH-D-12-00047.1, 2013.

Korolev, A. V., Isaac, G. A., and Hallett, J.: Ice particle habits in Arctic clouds, Geophysical Research Letters, 26, 1299–1302, 1999.

Korolev, A. V., Emery, E. F., Strapp, J. W., Cober, S. G., Isaac, G. A., Wasey, M., and Marcotte, D.: Small ice particles in tropospheric clouds: Fact or artifact? Airborne icing instrumentation evaluation experiment, Bulletin of the American Meteorological Society, 92, 967–973, https://doi.org/10.1175/2010BAMS3141.1, 2011.

Krämer, M., Rolf, C., Luebke, A., Afchine, A., Spelten, N., Costa, A., Meyer, J., Zoeger, M., Smith, J., Herman, R. L., Buchholz, B., Ebert, V., Baumgardner, D., Borrmann, S., Klingebiel, M., and Avallone, L.: A microphysics guide to cirrus clouds-Part 1: Cirrus types, Atmospheric Chemistry and Physics, 16, 3463–3483, https://doi.org/10.5194/acp-16-3463-2016, 2016.

Kuhn, T. and Heymsfield, A. J.: In Situ Balloon-Borne Ice Particle Imaging in High-Latitude Cirrus, Pure and Applied Geophysics, 173, 3065–3084, https://doi.org/10.1007/s00024-016-1324-x, 2016.

Kuhn, T., Heymsfield, A. J., and Buehler, S. A.: Balloon-borne measurements of ice particle shape and ice water content in the upper troposphere over Northern Sweden, in: European Space Agency, (Special Publication) ESA SP, vol. 721 SP, pp. 93–97, 2013.

Kuhn, T., Wolf, V., Völger, P., Stanev, M., and Gumbel, J.: Comparison of in-situ balloon-borne and lidar measurement of cirrus clouds, Proc. 23rd ESA Symposium on European Rocket and Balloon Programmes and Related Research, http://pac.spaceflight.esa.int/docs/23%20PAC%20Symposium.zip, 2017.

Lawson, P., O'Connor, D., Zmarzly, P., Weaver, K., Baker, B., Mo, Q., and Jonsson, H.: The 2DS (Stereo) Probe: Design and preliminary tests of a new airborne, high speed, high-resolution particle imaging probe, J. Atmos. Oceanic Technol., 2006.

Lawson, R. P., Baker, B. A., Schmitt, C. G., and Jensen, T. L.: An overview of microphysical properties of Arctic clouds observed in May and July 1998 during FIRE ACE, Journal of Geophysical Research Atmospheres, 106, 14 989–15 014, 2001.

Lindqvist, H., Muinonen, K., Nousiainen, T., Um, J., McFarquhar, G. M., Haapanala, P., Makkonen, R., and Hakkarainen, H.: Ice-cloud particle habit classification using principal components, Journal of Geophysical Research Atmospheres, 117, https://doi.org/10.1029/2012JD017573, 2012.

Liou, K.: Influence of cirrus clouds on weather and climate processes: a global perspective., Monthly Weather Review, 114, 1167–1199, 1986.

Luebke, A. E., Afchine, A., Costa, A., Grooss, J. U., Meyer, J., Rolf, C., Spelten, N., Avallone, L. M., Baumgardner, D., and Kraemer, M.: The origin of midlatitude ice clouds and the resulting influence on their microphysical properties, Atmospheric Chemistry and Physics, 16, 5793–5809, https://doi.org/10.5194/acp-16-5793-2016, 2016.

Lynch, D. K.: Cirrus, Oxford University Press, Cambridge ; New York, edited by David K. Lynch ... [et al.].; Includes bibliographical references and index., 2002.

Platt, C. M. R.: The role of cloud microphysics in high-cloud feedback effects on climate change, Nature, 341, 428–429, 1989.

Potter, G. L. and Cess, R. D.: Testing the impact of clouds on the radiation budgets of 19 atmospheric general circulation models, Journal of Geophysical Research D: Atmospheres, 109, 9, 2004.

Sassen, K. and Comstock, J. M.: A midlatitude cirrus cloud climatology from the facility foratmospheric remote sensing. Part III: Radiative properties, Journal of the Atmospheric Sciences, 58, 2113–2127, https://doi.org/AMCCCF>2.0.CO;2, 2001.

Schlimme, I., Macke, A., and Reichardt, J.: The impact of ice crystal shapes, size distributions, and spatial structures of cirrus clouds on solar radiative fluxes, Journal of the Atmospheric Sciences, 62, 2274–2283, https://doi.org/10.1175/JAS3459.1, 2005.

Schmitt, C. G., Iaquinta, J., and Heymsfield, A. J.: The asymmetry parameter of cirrus clouds composed of hollow bullet Rosette-shaped ice crystals from ray-tracing calculations, Journal of Applied Meteorology and Climatology, 45, 973–981, https://doi.org/10.1175/JAM2384.1, 2006.

Solomon, S., on Climate Change, I. P., and Intergovernmental Panel on Climate Change Working Group, I.: Climate change 2007: the physical science basis : contribution of Working Group I to the Fourth Assessment Report of the Intergovernmental Panel on Climate Change, Cambridge University Press, Cambridge ; New York, 2007.

Spichtinger, P., Gierens, K., and Drnbrack, A.: Formation of ice supersaturation by mesoscale gravity waves, Atmospheric Chemistry and Physics, 5, 1243–1255, 2005.

Tang, G., Panetta, R. L., Yang, P., Kattawar, G. W., and Zhai, P. W.: Effects of ice crystal surface roughness and air bubble inclusions on cirrus cloud radiative properties from remote sensing perspective, Journal of Quantitative Spectroscopy and Radiative Transfer, 195, 119–131, https://doi.org/10.1016/j.jqsrt.2017.01.016, 2017.

Voelger, P. and Nikulin, G.: The new lidar system at the Swedish Institute of Space Physics in Kiruna: description and first measurements, ESA-SP 590, 590, 321–325, 2005.

Weickmann, H., Sutton, M., of Supply, G. B. M., and Britain), R. A. E. G.: The Ice Phase in the Atmosphere, Ministry of Supply, https://books.google.se/books?id=D1mQHAAACAAJ, 1948.

Wernli, H., Boettcher, M., Joos, H., Miltenberger, A. K., and Spichtinger, P.: A trajectory-based classification of ERA-Interim ice clouds in the region of the North Atlantic storm track, Geophysical Research Letters, 43, 6657–6664, https://doi.org/10.1002/2016GL068922, 2016.